Aragonite saturation state dynamics in a coastal upwelling zone

Katherine E. Harris,[1] Michael D. DeGrandpre,[1] and Burke Hales[2]

Received 11 February 2013; revised 8 April 2013; accepted 9 April 2013; published 6 June 2013.

[1] Coastal upwelling zones may be at enhanced risk from ocean acidification as upwelling brings low aragonite saturation state (Ω_{Ar}) waters to the surface that are further suppressed by anthropogenic CO_2. Ω_{Ar} was calculated with pH, pCO_2, and salinity-derived alkalinity time series data from autonomous pH and pCO_2 instruments moored on the Oregon shelf and shelf break during different seasons from 2007 to 2011. Surface Ω_{Ar} values ranged between 0.66 ± 0.04 and 3.9 ± 0.04 compared to an estimated pre-industrial range of 1.0 ± 0.1 to 4.7 ± 0.1. Upwelling of high-CO_2 water and subsequent removal of CO_2 by phytoplankton imparts a dynamic range to Ω_{Ar} from ~1.0 to ~4.0 between spring and autumn. Freshwater input also suppresses saturation states during the spring. Winter Ω_{Ar} is less variable than during other seasons and is controlled primarily by mixing of the water column. **Citation:** Harris, K. E., M. D. DeGrandpre, and B. Hales (2013), Aragonite saturation state dynamics in a coastal upwelling zone, *Geophys. Res. Lett.*, *40*, 2720–2725, doi:10.1002/grl.50460.

1. Introduction

[2] The oceanic uptake of anthropogenic CO_2 and the resultant ocean acidification have been well-documented [*Haugan and Drange*, 1996; *Caldeira and Wickett*, 2003; *Feely et al*., 2009; *Midorikawa et al*., 2012], with a decrease in seawater pH of ~0.13 since pre-industrial times [*Dore et al*., 2009] and an accompanying decrease in the saturation state of calcium carbonate minerals. For aragonite, the more soluble form of $CaCO_3$, saturation state (Ω_{Ar}) is calculated using the relationship:

$$\Omega_{Ar} = \left[Ca^{2+}\right]\left[CO_3^{2-}\right]/K^*_{spAr} \quad (1)$$

where K^*_{spAr} is the apparent solubility product constant for aragonite. When $\Omega_{Ar} < 1$, waters are undersaturated and dissolution is thermodynamically favored. Although there are some exceptions [e.g., *Byrne et al*., 2009; *Dupont et al*., 2010; *Pansch et al*., 2012], most studies have determined that constant exposure to undersaturated waters can impair the health of many marine calcifiers [*Shirayama and Thornton*, 2005; *Gazeau et al*., 2007; *Fabry et al*., 2008; *Barton et al*., 2012; *Comeau et al*., 2012].

[3] Coastal upwelling zones, such as the one along the U.S. Pacific coast, naturally experience low Ω_{Ar} values as Ekman transport pumps subsurface water onto the shelf during periods of equatorward winds [*Hales et al*., 2005a; *Feely et al*., 2008; *Cao et al*., 2011; *Fassbender et al*., 2011]. These upwelling events also bring nutrients into the euphotic zone [*Hales et al*., 2005b]; and as a result, coastal upwelling zones are some of the most biologically productive in the world [*Muller-Karger et al*., 2005]. The resultant commercial fisheries are economically important [*Chavez and Messie*, 2009] and therefore ocean acidification could have important implications for both the marine ecosystem and the fisheries economy in these areas [*Barton et al*., 2012]. In the spring of 2007, *Feely et al*. [2008] found evidence of aragonite-undersaturated waters reaching the surface during strong upwelling along the coast of Northern California. A shellfish hatchery on the Oregon Coast also observed low Ω_{Ar} during the summer of 2009 [*Barton et al*., 2012]. With limited shipboard data, *Hales et al*. [2005a] showed that productivity on the shelf led to widespread depletions of surface water partial pressure of CO_2 (pCO_2) following upwelling events; however, *Evans et al*. [2011] found with moored time series measurements that offshore displacement of the productivity bloom associated with strong summer upwelling led to persistent high-pCO_2 in inner-shelf surface waters, suggesting that upwelling can depress surface Ω_{Ar} over extended periods and spatial areas.

[4] Shipboard studies have been important for mapping spatial distributions in Ω_{Ar} [e. g., *Hales et al*., 2005a; *Feely et al*., 2008; *Bates et al*., 2009; *Jiang et al*., 2010; *Cao et al*., 2011; *Fassbender et al*., 2011], but the seasonal variability and magnitude of Ω_{Ar} have not been well-characterized. *Juranek et al*. [2009, 2011] and *Alin et al*. [2012] have made important progress in estimating Ω_{Ar} using the more widespread oxygen and temperature (T) data, but these empirical relationships are only useful for waters >30 m depth. Autonomous sensors for two carbonate system parameters, pCO_2 and pH, are now available [*DeGrandpre et al*. 1995, 1999; *Seidel et al*, 2008], and extended time series studies can now be conducted on ocean moorings [*Gray et al*., 2011, 2012]. These data make it possible to calculate and characterize the daily, seasonal, and annual variation in Ω_{Ar} of highly dynamic regions like the Oregon shelf.

[5] As a follow-up to the air-sea CO_2 flux time series study by *Evans et al*. [2011], we present long-term time series of Ω_{Ar} values in the Oregon coastal upwelling zone. Additionally, we use high temporal resolution data to examine the processes controlling short-term changes in Ω_{Ar} and compare the current Ω_{Ar} range to the estimated pre-industrial Ω_{Ar} range.

2. Methods

[6] Seawater pCO_2 and pH were measured with Submersible Autonomous Moored Instruments for pCO_2 and pH (SAMI-CO_2 and SAMI-pH) [*DeGrandpre et al*., 1995,

Additional supporting information may be found in the online version of this article.

[1]Department of Chemistry and Biochemistry, The University of Montana, Missoula, Montana, USA.
[2]College of Earth, Ocean, and Atmospheric Sciences, Oregon State University, Corvallis, Oregon, USA.

Corresponding author: M. D. DeGrandpre, Department of Chemistry and Biochemistry, 32 Campus Dr., The University of Montana, Missoula, MT 59812, USA. (michael.degrandpre@umontana.edu)

0094-8276/13/10.1002/grl.50460

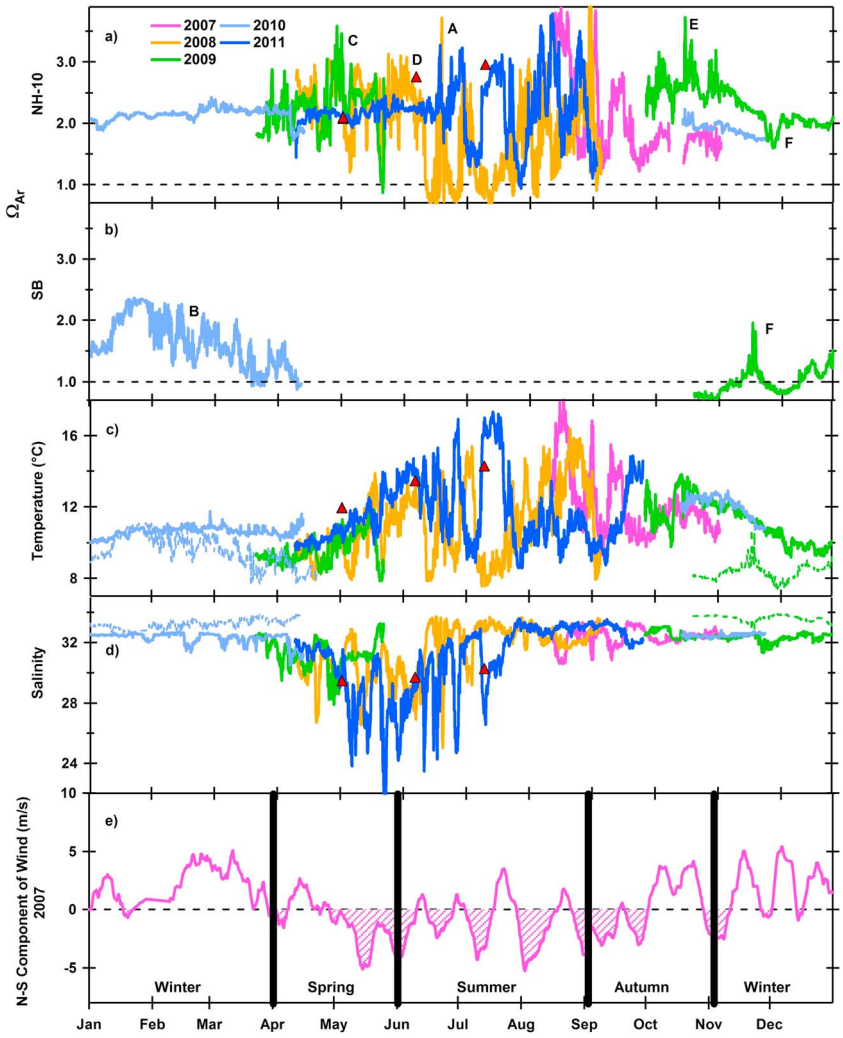

Figure 1. Ω_{Ar} time series at (a) NH-10 (2 m depth) and (b) shelf break (SB) (116 m depth). Refer to the legend in Figure 1a for all Figure 1 color schemes. $\Omega_{Ar} = 1$ (dashed black). The filled red triangles represent discrete samples taken from surface waters near NH-10 (see supporting information). (c) Temperature at NH-10 (solid) and SB (dashed). (d) Salinity at NH-10 (solid) and SB (dashed). (e) 10 day averaged N-S component of wind for 2007 to show seasonal upwelling (negative values, equatorward winds) and downwelling (positive values, poleward winds). The wind data from 2008 to 2011 are found in the supporting information (Figure S1). Seasons are indicated in Figure 1e according to the division of seasons on the shelf used by *Smith et al*. [2001].

1999; *Seidel et al*., 2008]. The data presented here are from instruments deployed at 2 m depth on the NH-10 buoy located on the 80 m isobath ~20 km from shore (124.304°W, 44.633°N) and at 116 m depth on the shelf break (SB) mooring located on the 120 m isobath ~35 km offshore (124.500°W, 44.641°N) along the Newport Hydrographic (NH) Line. From 2007 to 2008, only SAMI-CO_2 instruments were deployed. From 2009 to 2011, SAMI-CO_2 and SAMI-pH pairs were deployed on NH-10. Due to various problems, combined pCO_2 and pH data were obtained only for spring 2009, autumn 2009, and from spring to early summer 2011. Saturation states, dissolved inorganic carbon (DIC), and other carbonate parameters were calculated in CO2SYS [*Pierrot et al*., 2006] using a combination of pH or pCO_2 data and salinity-derived alkalinity (A_{Tsalin}). A_{Tsalin} can be calculated using the relationship reported by *Gray et al*. [2011] for the U.S. Pacific coast. As shown by *Gray et al*. [2011], A_{Tsalin} combined with pH or pCO_2 can provide better estimates of Ω_{Ar} than the pH-pCO_2 combination. The validity of the A_{Tsalin} relationship is checked by comparing the measured pH with that calculated from the A_{Tsalin}-pCO_2 combination when both pH and pCO_2 data were available. Based on this comparison, we found that the relationship in *Gray et al*. [2011] predicts A_T with reasonable accuracy. The average differences for all periods when pH and pCO_2 were available ranged from 0.01 ± 0.02 for pH to 7 ± 12 µatm for pCO_2, which led to an average difference in calculated Ω_{Ar} of 0.04 ± 0.08. Further discussion of these uncertainties can be found in the supporting information.

[7] The processes controlling Ω_{Ar} dynamics were analyzed using property:property plots of Ω_{Ar} versus DIC or salinity (S) with reaction pathways super-imposed for net community production (NCP), air-sea gas exchange, water mass mixing, and dilution by river run-off. In brief, the NCP reaction pathway in the Ω_{Ar}:DIC plot was derived by varying DIC and A_T in proportion to the Redfield ratio (106:18). Changes in Ω_{Ar} due to mixing of shelf water with

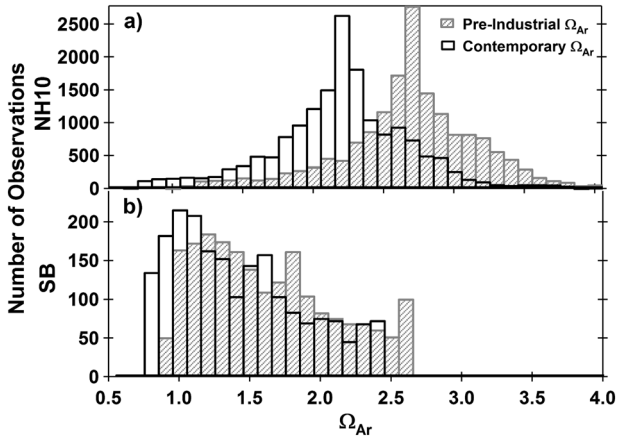

Figure 2. Frequency distribution of Ω_{Ar} for (a) NH-10 and (b) the shelf break (SB). Data from 2007 to 2011 are represented by the unfilled bars, and pre-industrial Ω_{Ar} values are represented by the cross hatched bars.

the Columbia River (CR) plume were represented by a simple two end-member mixing model. The effect of air-sea gas exchange was modeled by incrementing the mean DIC by the air-sea CO_2 flux keeping A_T constant.

[8] The Ω_{Ar} time series were compared to pre-industrial Ω_{Ar} estimated using the difference between current and pre-industrial pCO_2 based on a method modified from *Feely et al*. [2008]. The supporting information provides additional details on the methods used for this study.

3. Results

[9] The multi-year time series for Ω_{Ar}, S, and T are plotted in Figure 1, along with the North-South component of the winds from 2007 to show seasonal changes in upwelling and downwelling. The pCO_2 and pH data, along with winds from 2008 to 2011, can be found in the supporting information (Figure S1). Surface Ω_{Ar} ranged from 0.66 to 3.9 (Figure 1a, Figure 2). The mean Ω_{Ar} was 2.2 ± 0.5, significantly below the estimated average for the North Pacific Ocean (3.3 ± 0.7) [*Feely et al*., 2009]. Ω_{Ar} was highly variable in all seasons except winter. The greatest temporal variability occurred during the summer upwelling season (Figure 1a, June through August) as periods of strong upwelling-favorable winds alternated with relaxation events (Figure 1e). In one event, surface water Ω_{Ar} changed by ~3 over a diel period (mid-June 2008, Figure 1a, point A). There were seven intervals of $\Omega_{Ar} < 1$ (Figure 1a) on the surface at NH-10 that persisted from 6 h to 3 days, although the frequency and duration of upwelling events differed inter-annually. In their study of Netarts Bay (2 m average depth) on the Oregon coast, *Barton et al*. [2012] found frequent periods of undersaturation during summer 2009, a result of the stronger influence of upwelling near shore, as well as contributions from nighttime net respiration in shallow sediments of the bay.

[10] Average Ω_{Ar} values in SB bottom boundary layer waters were 1.4 ± 0.5, nearly one unit lower than values seen at the surface during the same time period (Figures 1b and 2). Due to remote wind forcing, low Ω_{Ar} waters (Figure 1b, point B) appeared long before local winds indicated upwelling-favorable conditions. The periods of low saturation support the seasonal dynamics of Ω_{Ar} predicted for SB waters by *Juranek et al*. [2009]. Unlike the near-Gaussian distribution seen in surface Ω_{Ar} (Figure 2), the deep SB water was constrained by the lower Ω_{Ar} of the California Undercurrent end-member, estimated to be 0.9 ± 0.3 from mean California Undercurrent T, S, DIC, and alkalinity (A_T) (see supporting information).

4. Discussion

[11] Several processes contribute to Ω_{Ar} variability on the shelf including upwelling and other water mass changes (e.g., riverine inputs), NCP, and air-sea gas exchange. Variability from $CaCO_3$ formation and dissolution is expected to be minimal in this area [*Fassbender et al*., 2011]. We plotted Ω_{Ar} versus DIC and S (Figure 3) to discern relative contributions from each mechanism, calculated as described in section 2 and supporting information.

[12] Several of these processes were important but varied widely between seasons and from year to year (Figure 3). Spring data are discussed first with interannual variability when applicable. Spring (April–May, 2008–2010) variability generally followed NCP and gas exchange relationships (Figure 3a). Surface Ω_{Ar} values extended along the Redfield relationship from low Ω_{Ar} (0.8–1.3) and high DIC indicative of the SB end-member to high Ω_{Ar} (>3.0) and low DIC as nutrient-rich upwelled waters triggered biological DIC uptake and drove Ω_{Ar} up. Biological production uses up the excess preformed nutrients that accompany the upwelled water [*Hales et al*., 2005a, 2005b], and surface water pCO_2 can be driven well below atmospheric saturation, thereby increasing Ω_{Ar} and extending the original Redfield signature of the upwelled SB water (Figure 3a, SB data in 3g). Spring 2011 exhibited strong effects of CR dilution relative to the previous springs as Ω_{Ar} was depressed due to dilution of $[Ca^{2+}]$ and $[CO_3^{2-}]$ by the CR plume (Figures 3a–3b) [*Salisbury et al*., 2008; *Chierici and Fransson*, 2009]. The CR plume regularly extends southward from the river mouth during spring and summer, although its width and distance from shore vary based on wind conditions and water discharge [*Hickey et al*., 2005; *Burla et al*., 2010]. Water gauge records for the Columbia River (Table S3, supporting information) indicate that the spring 2011 river discharge was 130–140% greater than that during spring 2008 and 2009. The higher discharge and weaker upwelling (as measured by upwelling index, Table S3) during this period resulted in a stronger influence of the CR plume relative to other years. The 2011 data do not exactly follow the CR dilution trend, and it is likely that NCP increased Ω_{Ar} (up to ~0.75) above the Ω_{Ar} predicted by the CR dilution trend (Figures 3a and 3b). *Fassbender et al*. [2011] examined DIC dynamics on the U.S. West Coast using cruise data from two Northern California shelf transects during May 2007. They used a box model to estimate the effect of primary productivity on inorganic carbon dynamics and found that full utilization of available nitrate would result in a sea surface Ω_{Ar} of ~3. This value is comparable to the maximum spring sea surface Ω_{Ar} values observed at NH-10 (Figure 1a, points C and D; Figure 3a, 2008, 2009), supporting the importance of NCP in regulating Ω_{Ar} on the shelf.

[13] Relationships between Ω_{Ar}, DIC, and S during summer (June–August, 2008 and 2011) (Figures 3c–3d) are similar to those observed for the spring. In 2008 and 2011, the strong influence of the CR plume due to weaker upwelling and higher CR discharge (compared to 2010, Table S3) additionally suppressed Ω_{Ar} already lowered by upwelling.

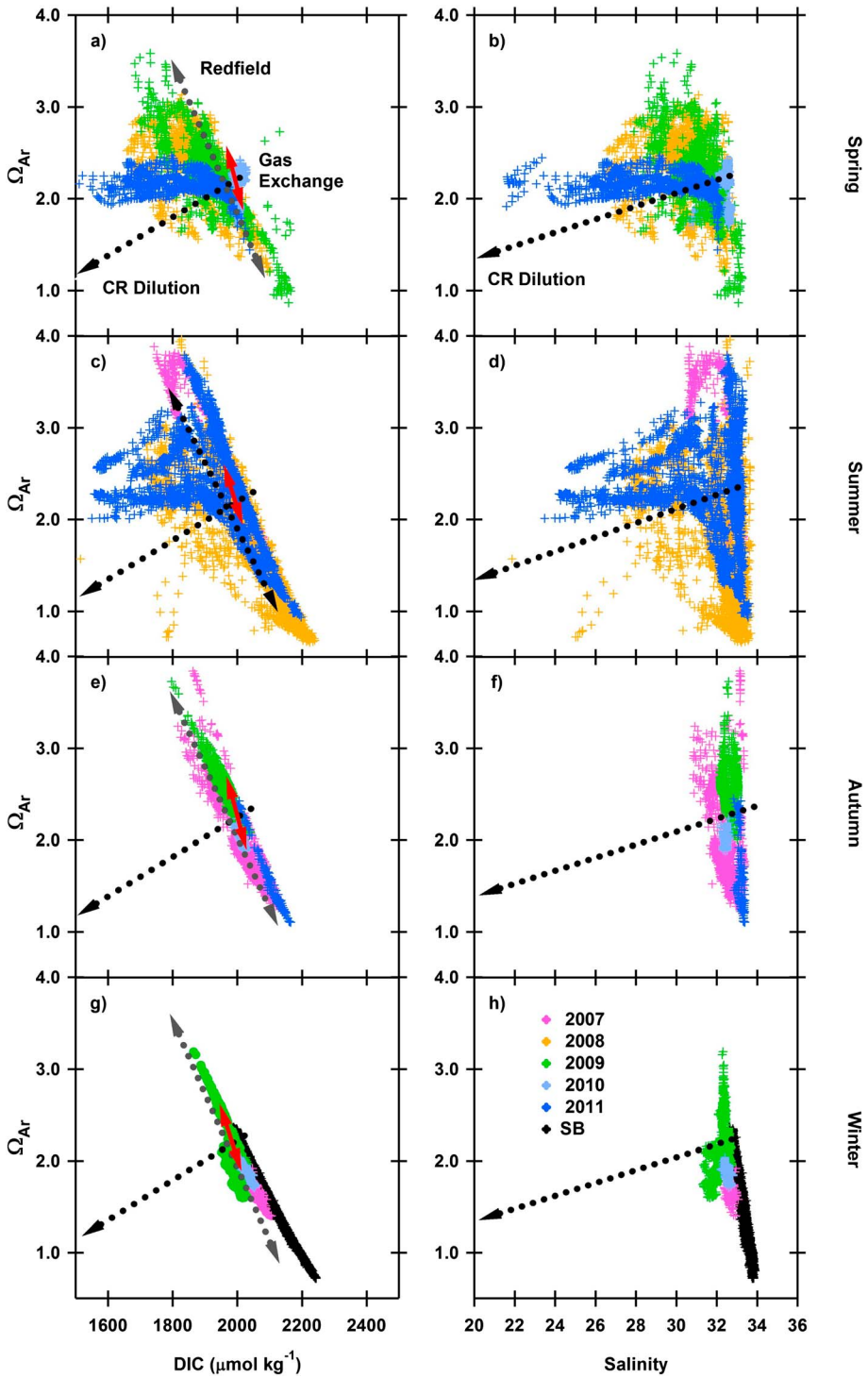

Figure 3. The relationships between Ω_{Ar} and DIC (calculated as described in the supporting information) and salinity during each season (labeled at right). (a,c,e,g) The Redfield (gray), (a,c,e,g) gas exchange (red), and (a–h) Columbia River dilution (black). The magnitude of the arrows corresponds to each relationship's potential effect on Ω_{Ar}. Years are identified by the color legend in lower right corner. Winter 2009 includes data from November 2009 through March 2010. The SB data are from November 2009 to March 2010.

[14] Trends in Ω_{Ar} in autumn (September–October) (Figures 3e–3f) and early winter (Figures 3g–3h) closely followed the predicted trends in biological productivity and gas exchange (Figures 3e and 3g) with little evidence of the dilution effects seen in spring and summer. In autumn 2009, the Ω_{Ar} was high (>3.0, Figure 1a, point E) but began to decline, likely due to convective mixing of the water column. In mid- to late November 2009, the mixed layer depth (MLD, not shown) deepened from near 25 m to >70 m, mixing surface and subpycnocline water and lowering surface Ω_{Ar}. Winter SB and NH-10 Ω_{Ar} relationships overlapped as a result of the homogenized water column (Figures 1a and 1b, point F;

Figures 3g and 3h). After this period, surface Ω_{Ar} varied little for the remainder of winter 2009, with an average of 2.2 ± 0.4. Autumn 2010 Ω_{Ar} was significantly lower than in 2009 as a result of the prolonged and intense summer upwelling (wind data shown in Figures S1e and S1f).

[15] Winter SB Ω_{Ar} (the only season when SB data were collected) was mainly influenced by vertical mixing, downwelling, and movement of upwelled water onto the shelf driven by remote wind forcing [*Hickey et al*., 2006] (Figures 3g and 3h). There was little short-term variability in comparison to the surface data because these bottom waters were not influenced by gas exchange, heating or cooling, or the CR plume to any significant extent.

5. Implications

[16] These inorganic carbon data were used to back-calculate the natural (i.e., pre-industrial) Ω_{Ar} range on the shelf (see supporting information). This analysis indicates that mean contemporary Ω_{Ar} is 0.52 less than mean pre-industrial levels (Figure 2). Pre-industrial Ω_{Ar} was rarely undersaturated whereas contemporary surface values occasionally drop as low as 0.66. At the shelf break, contemporary Ω_{Ar} is undersaturated ~30% of the time, whereas pre-industrial undersaturation occurred only ~10% of the time. These changes in Ω_{Ar} from pre-industrial levels are consistent with the findings of the modeled simulations of *Hauri et al*. [2013] which also concluded that contemporary Ω_{Ar} observations in the California Current System have already shifted substantially from the pre-industrial range. It is unclear to what extent the shift to lower saturation in surface waters is affecting local organisms, all of which evolved in pre-industrial conditions. Reductions in Ω_{Ar}, even for waters that remain supersaturated, have been shown to harm many aragonite-forming organisms, resulting in shell dissolution for pteropods [*Bednaršek et al*., 2012; *Comeau et al*., 2012], decreased larval and mid-stage growth rates in bivalves [*Gazeau et al*., 2007; *Barton et al*., 2012; G. G. Waldbusser et al., A developmental and energetic basis linking larval oyster shell formation to acidification sensitivity, accepted by *Geophysical Research Letters*, 2013], and lower developmental rates in echinoderms [*Shirayama and Thornton*, 2005; *O'Donnell et al*., 2010]. Researchers that conduct ocean acidification-related organismal studies should consider the range of variability in this study when developing experimental designs. In addition, this study suggests that Ω_{Ar} can be calculated with reasonable accuracy from previously collected high-frequency pH or pCO_2 data if salinity was also measured and the relationship with alkalinity is known.

[17] With atmospheric CO_2 concentrations continuing to rise and an increasing trend in upwelling wind strength and duration [*Bakun*, 1990; *Schwing and Mendelssohn*, 1997; *McGregor et al*., 2007], it is likely that periods of undersaturation will increase in both frequency and intensity. Therefore, long-term monitoring of ocean saturation states will continue to be necessary.

[18] **Acknowledgments.** We thank C. Beatty (The University of Montana), C. Holm, M. Levine, D. Hubbard, D. Langner, and C. Wall (Oregon State University) for help with the SAMI deployments, and the OrCOOS program for the buoy. We thank the two reviewers for their constructive and detailed comments. This research was funded by the National Science Foundation (OCE-0836807 and OCE-0628569) and a NASA Space Grant Consortium Fellowship to K. E. Harris.

[19] The Editor thanks two anonymous reviewers for their assistance in evaluating this paper.

References

Alin, S. R., R. A. Feely, A. G. Dickson, J. M. Hernandez-Ayon, L. W. Juranek, M. D. Ohman, and R. Goericke (2012), Robust empirical relationships for estimating the carbonate system in the southern California Current System and application to CalCOFI hydrographic cruise data (2005–2011), *J. Geophys. Res.*, *117*, C05033, doi:10.1029/2011JC007511.

Bakun, A. (1990), Global climate change and intensification of coastal ocean upwelling, *Science*, *247*(4939), 198–201, doi:10.1126/science.247.4939.198.

Barton, A., B. Hales, G. C. Waldbusser, C. Langdon, and R. A. Feely (2012), The Pacific oyster, *Crassostrea gigas*, shows negative correlation to naturally elevated carbon dioxide levels: Implications for near-term ocean acidification effects, *Limnol. Oceanogr.*, *57*(3), 698–710, doi:10.4319/lo.2012.57.3.0698.

Bates, N. R., J. T. Mathis, and L. W. Cooper (2009), Ocean acidification and biologically induced seasonality of carbonate mineral saturation states in the western Arctic Ocean, *J. Geophys. Res.*, *114*, C11007, doi:10.1029/2008JC004862.

Bednaršek, N., et al. (2012), Extensive dissolution of live pteropods in the Southern Ocean, *Nat. Geosci.*, *5*, 881–885, doi:10.1038/ngeo1635.

Burla, M., A. M. Baptista, Y. L. Zhang, S. Frolov (2010), Seasonal and interannual variability of the Columbia River plume: A perspective enabled by multiyear simulation databases, *J. Geophys. Res.*, *115*, C00B16, doi:10.1029/2008JC004964.

Byrne, M., M. Ho, P. Selvakumaraswamy, H. D. Nguyen, S. A. Dworjanyn, and A. R. Davis (2009), Temperature, but not pH, compromises sea urchin fertilization and early development under near-future climate change scenarios, *Proc. R. Soc. B*, *276*(1663), 1883–1888, doi:10.1098/rspb.2008.1935.

Caldeira, K., and M. E. Wickett (2003), Oceanography: Anthropogenic carbon and ocean pH, *Nature*, *425*(6956), 365, doi:10.1038/425365a.

Cao, Z., M. H. Dai, N. Zheng, D. L. Wang, Q. Li, W. D. Zhai, F. F. Meng, and J. P. Gan (2011), Dynamics of the carbonate system in a large continental shelf system under the influence of both a river plume and coastal upwelling, *J. Geophys. Res.*, *116*, G02010, doi:10.1029/2010JG001596.

Chavez, F. P., and M. Messie (2009), A comparison of Eastern Boundary Upwelling Ecosystems, *Prog. Oceanogr.*, *83*(1–4), 80–96, doi:10.1016/j.pocean.2009.07.032.

Chierici, M., and A. Fransson (2009), Calcium carbonate saturation in the surface water of the Arctic Ocean: Undersaturation in freshwater influenced shelves, *Biogeosci.*, *6*(11), 2421–2431, doi:10.5194/bg-6-2421-2009.

Comeau, S., J. P. Gattuso, A. M. Nisumaa, and J. Orr (2012), Impact of aragonite saturation state changes on migratory pteropods, *Proc. R. Soc. B*, *279*(1729), 732–738, doi:10.1098/rspb.2011.0910.

DeGrandpre, M. D., T. R. Hammar, S. P. Smith, and F. L. Sayles (1995), In-situ measurements of seawater pCO_2, *Limnol. Oceanogr.*, *40*(5), 969–975.

DeGrandpre, M. D., M. M. Baehr, and T. R. Hammar (1999), Calibration-free optical chemical sensors, *Anal. Chem.*, *71*(6), 1152–1159, doi:10.1021/ac9805955.

Dore, J. E., R. Lukas, D. W. Sadler, M. J. Church, and D. M. Karl (2009), Physical and biogeochemical modulation of ocean acidification in the central North Pacific, *Proc. Natl. Acad. Sci. USA*, *106*(30), 12235–12240, doi:10.1073/pnas.0906044106.

Dupont, S., B. Lundve, and M. Thorndyke (2010), Near future ocean acidification increases growth rate of the lecithotrophic larvae and juveniles of the sea star *Crassaster papposus*, *J. Exp. Zool, Part B.*, *314B*(5), 382–389, doi:10.1002/jezmde.21342.

Evans, W., B. Hales, and P. G. Strutton (2011), Seasonal cycle of surface ocean pCO_2 on the Oregon shelf, *J. Geophys. Res.*, *116*, C05012, doi:10.1029/2010JC006625.

Fabry, V. J., B. A. Seibel, R. A. Feely, and J. C. Orr (2008), Impacts of ocean acidification on marine fauna and ecosystem processes, *ICES J. Mar. Sci.*, *65*(3), 414–432, doi:10.1093/icesjms/fsn048.

Fassbender, A. J., C. L. Sabine, R. A. Feely, C. Langdon, and C. W. Mordy (2011), Inorganic carbon dynamics during northern California coastal upwelling, *Cont. Shelf Res.*, *31*(11), 1180–1192, doi:10.1016/j.csr.2011.04.006.

Feely, R. A., C. L. Sabine, J. M. Hernandez-Ayon, D. Ianson, and B. Hales (2008), Evidence for upwelling of corrosive "acidified" water onto the continental shelf, *Science*, *320*(5882), 1490–1492, doi:10.1126/science.1155676.

Feely, R. A., S. C. Doney, and S. R. Cooley (2009), Ocean acidification: Present conditions and future changes in a high-CO_2 world, *Oceanogr.*, *22*(4), 36–47, doi:10.5670/oceanog.2009.95.

Gazeau, F., C. Quiblier, J. M. Jansen, J. P. Gattuso, J. J. Middelburg, and C. H. R. Heip (2007), Impact of elevated CO_2 on shellfish calcification, *Geophys. Res. Lett.*, *34*, L07603, doi:10.1029/2006GL028554.

Gray, S. E. C., M. D. DeGrandpre, T. S. Moore, T. R. Martz, G. E. Friederich, and K. S. Johnson (2011), Applications of in situ pH measurements for

inorganic carbon calculations, *Mar Chem.*, *125*(1–4), 82–90, doi:10.1016/j.marchem.2011.02.005.

Gray, S. E. C., M. D. DeGrandpre, C. Langdon, and J. E. Corredor (2012), Short-term and seasonal pH, pCO_2 and saturation state variability in a coral-reef ecosystem, *Global Biogeochem. Cycles*, *26*, GB3012, doi:10.1029/2011GB004114.

Hales, B., J. N. Moum, P. Covert, and A. Perlin (2005a), Irreversible nitrate fluxes due to turbulent mixing in a coastal upwelling system, *J. Geophys. Res.*, *110*, C10S11, doi:10.1029/2004JC002685.

Hales, B., T. Takahashi, and L. Bandstra (2005b), Atmospheric CO_2 uptake by a coastal upwelling system, *Global Biogeochem. Cycles 19*, GB1009, doi:10.1029/2004GB002295.

Haugan, P. M., and H. Drange (1996), Effects of CO_2 on the ocean environment, *Energ. Convers. Manage*, *37*(6–8), 1019–1022, doi:10.1016/0196-8904(95)00292-8.

Hauri, C., N. Gruber, M. Vogt, S. C. Doney, R. A. Feely, Z. Lachkar, A. Leinweber, A. M. P. McDonnell, M. Munnich, and G.-K. Plattner (2013), Spatiotemporal variability and long-term trends of ocean acidification in the California Current System, *Biogeosci.*, *10*, 193–216, doi:10.5194/bg-10-193-2013.

Hickey, B., S. Geier, N. Kachel, and A. MacFadyen (2005), A bi-directional river plume: The Columbia in summer, *Cont. Shelf Res.*, *25*(14), 1631–1656, doi:10.1016/j.csr.2005.04.010.

Hickey, B., A. MacFadyen, W. Cochlan, R. Kudela, K. Bruland, C. Trick (2006), Evolution of chemical, biological, and physical water properties in the northern California Current in 2005: Remote or local wind forcing?, *Geophys. Res. Lett.*, *33*, L22S02, doi:10.1029/2006GL026782.

Jiang, L. Q., et al. (2010), Carbonate mineral saturation states along the US East Coast, *Limnol. Oceanogr.*, *55*(6), 2424–2432, doi:10.4319/lo.2010.55.6.2424.

Juranek, L. W., R. A. Feely, W. T. Peterson, S. R. Alin, B. Hales, C. L. Sabine, and J. Peterson (2009), A novel method for determination of aragonite saturation state on the continental shelf of central Oregon using multi-parameter relationships with hydrographic data, *Geophys. Res. Lett.*, *36*, L24601, doi:10.1029/2009GL040778.

Juranek, L. W., R. A. Feely, D. Gilbert, H. Freeland, and L. A. Miller (2011), Real-time estimation of pH and aragonite saturation state from Argo profiling floats: Prospects for an autonomous carbon observing strategy, *Geophys. Res. Lett.*, *38*, L17603, doi:10.1029/2011GL048580.

McGregor, H. V., M. Dima, H. W. Fischer, and S. Mulitza (2007), Rapid 20th-century increase in coastal upwelling off northwest Africa, *Science*, *315*(5812), 637–639, doi:10.1126/science.1134839.

Midorikawa, T., H. Y. Inoue, M. Ishii, D. Sasano, N. Kosugi, G. Hashida, S. Nakaoka, and T. Suzuki (2012), Decreasing pH trend estimated from 35-year time series of carbonate parameters in the Pacific sector of the Southern Ocean in summer, *Deep-Sea Res I.*, *61*, 131–139, doi:10.1016/j.dsr.2011.12.003.

Muller-Karger, F. E., R. Varela, R. Thunell, R. Luerssen, C. M. Hu, J. J. Walsh (2005), The importance of continental margins in the global carbon cycle, *Geophys. Res. Lett.*, *32*, L01602, doi:10.1029/2004GL021346.

O'Donnell, M. J., A. E. Todgham, M. A. Sewell, L. M. Hammond, K. Ruggiero, N. A. Fangue, M. L. Zippay, and G. E. Hoffman (2010), Ocean acidification alters skeletogenesis and gene expression in larval sea urchins, *Mar. Ecol. Prog.*, *398*, 151–171, doi:10.3354/meps08346.

Pansch, C., A. Nasroiahi, Y. S. Appelhans, and M. Wahl (2012), Impacts of ocean warming and acidification on the larval development of the barnacle *Amphibalanus improvisus*, *J. Exp. Mar. Biol. Ecol.*, *420*, 48–55, doi:10.1016/jembe.2012.03.023.

Pierrot, D., E. Lewis, and D. W. R. Wallace (2006), MS Excel program developed for CO2 system calculations, ORNL/CDIAC-105a, U.S. Dep. of Energy, Oak Ridge, Tenn., doi:10.3334/CDIAC/otg.CO2SYS_XLS_CDIAC105a.

Salisbury, J., M. Green, C. Hunt, and J. Campbell (2008), Coastal acidification by rivers: A threat to shellfish?, *Eos Trans. AGU*, *89*(50), 513–514, doi:10.1029/2008EO500001.

Schwing, F. B., and R. Mendelssohn (1997), Increased coastal upwelling in the California Current System, *J. Geophys. Res.*, *102*(C2), 3421–3438, doi:10.1029/96JC03591.

Seidel, M. P., M. D. DeGrandpre, and A. G. Dickson (2008), A sensor for in situ indicator-based measurements of seawater pH, *Mar. Chem.*, *109*(1–2), 18–28, doi:10.1016/j.marchem.2007.11.013.

Shirayama, Y., and H. Thornton (2005), Effect of increased atmospheric CO_2 on shallow water marine benthos, *J. Geophys. Res.*, *110*, C09S08, doi:10.1029/2004JC002618.

Smith, C. L., A. E. Hill, M. G. G. Foreman, and M. A. Pena (2001), Horizontal transport of marine organisms resulting from interactions between diel vertical migration and tidal currents off the west coast of Vancouver Island, *Can. J. Fish. Aquat. Sci.*, *58*(4), 736–748, doi:10.1139/cjfas-58-4-736.